16th European Signal Processing Conference (EUSIPCO 2008), Lausanne, Switzerland, August 25-29, 2008, copyright by EURASIP

REMOVAL OF CORRELATED RICIAN NOISE IN MAGNETIC RESONANCE IMAGING

Jan Aelterman, Bart Goossens, Aleksandra Pižurica and Wilfried Philips

Ghent University - TELIN - IPI - IBBT
St.-Pietersnieuwstraat 41, B-9000 Gent, Belgium
email: Jan.Aelterman@Telin.Ugent.Be

ABSTRACT

We propose a new method for Magnetic Resonance Imaging (MRI) restoration. Because MR magnitude images are corrupted by Rician distributed noise, these images suffer from a contrast-reducing signal-dependent bias. Also the noise is often assumed to be white, however a widely used acquisition technique to decrease the acquisition time gives rise to correlated noise. In this paper, we propose and motivate a two-step denoising procedure, where bias is removed from the squared magnitude image and denoising itself is then performed on the square root of this image in the wavelet domain. This denoising step takes into account noise correlation when distinguishing significant wavelet coefficients from insignificant ones. The estimated statistics of these two classes of wavelet coefficients are employed within a Bayesian estimator. The results show that the proposed technique is more efficient at removing correlated noise than existing MRI denoising techniques. The presented bias removal technique is shown to visibly improve contrast as well as to provide a large increase in PSNR.

1. INTRODUCTION

Magnetic Resonance Imaging (MRI) has evolved significantly over the last few decades. With the rise of fast acquisition techniques, as used in e.g. functional MRI, ever increasing demands are being made of MRI technology. In practice, MRI signals are acquired in the K-space, which is the multi-dimensional frequency-space transformation of the ordinary Euclidian R-space. Reconstruction of the signal in spatial coordinates involves a discrete Fourier transform (DFT). The phase encoding procedure [1] does not result in complex conjugates for the corresponding positive and negative frequency values in the K-space. The reasons are noise and technical limitations in the system itself [2]. Therefore, R-space signal will be present in both orthogonal channels. To visualize this complex signal, many commercial MRI scanners show the magnitude image. Since the DFT is a unitary transform, the white Gaussian noise on the measured quadrature signals is converted into white Gaussian noise on the two orthogonal R-space signals. The magnitude of this complex signal corrupted by Gaussian noise then exhibits Rician distributed noise [2]. Hence, it is generally well accepted to model noise on magnitude MR images as white and Rician distributed [3, 4, 5]. There exist some techniques that are adapted to Rician noise [4, 6]. It has been shown that Rician noise is approximated very well by Gaussian noise in the case of high SNR (bright regions). Because of this, it should not surprise that some techniques perform well on magnitude MR images without taking the Rician nature into account [7]. However, in low SNR regions, the Rician noise distribution deviates significantly from the Gaussian one, also by introducing a bias with respect to the signal level. In [4], a method was proposed to remove this bias, while processing the squared magnitude image. We will present some drawbacks to this approach and propose a two-step denoising procedure in which these drawbacks are eliminated. Some authors suggest denoising complex data [8] as this circumvenes problems with Rician noise completely. However, complex data is not readily, if at all, available for postprocessing in practice.

This paper contributes by presenting a method for restoring MR magnitude images, that consists of a bias removal step on the squared magnitude image and a wavelet-based denoising step on the magnitude image. As we will show, the Rician noise becomes correlated because of a widely used technique to decrease acquisition time. Therefore, we measure the noise Power Spectral Density (PSD) and take it into account in our denoising algorithm. This leads to improvements both visually as in PSNR compared to existing MRI denoising techniques.

The remainder of this paper is organised as follows: In Section 2 we discuss the causes of noise correlations in MRI. In Section 3, we present our method for bias removal and noise suppression. Results and discussion are given in Section 4. Finally, Section 5 concludes this paper.

2. CORRELATIONS IN MRI NOISE

Most existing MRI denoising methods assume uncorrelated noise, which is justified for some MRI modalities. Figure 1(a) shows slice detail from a 3 Dimensional Time Of Flight (TOF) Magnetic Resonance Angiography (MRA) sequence. This type of sequence is typically used for imaging flowing blood inside arteries and veins of the body. To speed up the aquisition process for this sequence, the K-space is subsampled by reducing the number of phase encoding steps. Higher frequency information in K-space is not sampled (set to zero) before the inverse Fourier transform, so the technique comes down to sinc-interpolation of an image of lower resolution in the phase encoding direction. The operator is free to choose the subsampling factor which causes the aquisition time to be divided by this factor. The effect on the magnitude image is that the noise power spectral density (PSD) is cut off in the horizontal high frequencies. This is evident by the noise behaving as short

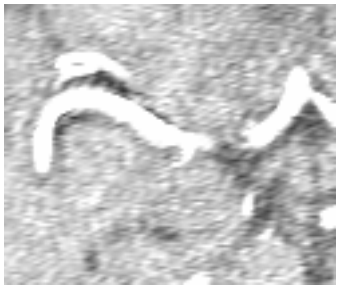

(a)

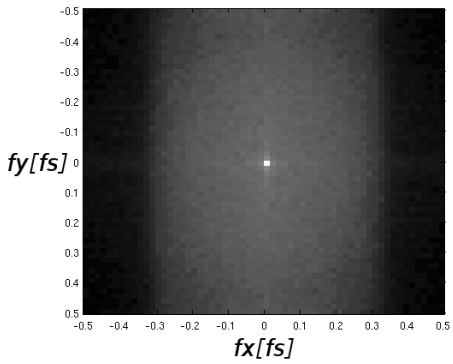

(b)

Figure 1: (a) Detail of a real MR magnitude image. (b) corresponding Noise Power Spectral Density averaged over all slices.

horizontal stripes. Furthermore, it is observed that this cutoff is not perfect in actual MRI. This makes it difficult to establish the exact cutoff frequency. Hence, it is not straightforward to reduce the MR image in resolution so that the noise becomes ideally white. We therefore develop a new denoising algorithm for correlated noise that operates on the original acquired image. The mentioned phase subsampling technique is not limited to 3D TOF MRA, but is available for most MRI sequences. This means that one can not always assume that the noise in magnitude MR images is white.

3. PROPOSED METHOD

3.1 Bias Removal

We will use the following noise model:

$$Y = A + N$$

where Y is the Rician distributed signal, A is the noiseless voxel value and N is the Rician noise. We can write the mean and variance of the Rician distributed signal Y as [3]:

$$\begin{aligned} E[Y] &= \sigma\sqrt{\frac{\pi}{2}} M\left(-\frac{1}{2}, 1, -\frac{A^2}{2\sigma^2}\right) \\ Var[Y] &= A^2 + 2\sigma^2 - \frac{\sigma^2\pi}{2} M^2\left(-\frac{1}{2}, 1, -\frac{A^2}{2\sigma^2}\right) \end{aligned}$$

where $M(\cdot,\cdot,\cdot)$ is the confluent hypergeometric function [9]. From this, we see that Y is indeed biased with respect to A and, to worsen the situation, the bias is signal-dependent: large for low SNR (dark regions) and small for high SNR (bright regions). As such, the bias reduces contrast between bright and dark areas, which is directly related to difference in tissue. Hence, contrast to noise (CNR) ratio is a very important factor in MRI systems, which motivates us to take a closer look at the introduced bias.

It can be verified that $M(-\frac{1}{2}, 1, -\frac{A^2}{2\sigma^2})$ quickly approaches $\frac{2A^2+\sigma^2}{\sqrt{2\pi}\sigma A}$ as the SNR becomes large [9], which removes the bias and sets the variance to σ^2. This agrees with the observation that the Rician distribution approaches a Gaussian one for high SNR. A chi-square test with significance of 0.01 shows that the Gaussian approximation is valid for $\frac{A}{\sigma} > 4$, which is true for most of the useful signal. In low SNR parts of the image, another approach is necessary, as the bias cannot be disregarded. In [4], a method is proposed to remove the bias, making use of the properties of the squared magnitude image, which is distributed according to a chi-square distribution with two degrees of freedom:

$$E\left[Y^2\right] = A^2 + 2\sigma^2 \quad (1)$$

$$Var\left[Y^2\right] = 4\sigma^4\left(\frac{A^2}{\sigma^2} + 1\right) \quad (2)$$

It is important to realize that (1) has a fixed, signal-independent bias. This property can be exploited to remove this bias, thus we can increase the image contrast, by substracting the bias from each pixel in the squared magnitude image:

$$\widehat{Y^2} = Y^2 - 2\hat{\sigma}^2 \quad (3)$$

Note however, that this does not remove the bias on the magnitude image completely, as the necessary square root operation introduces a new bias [3]. Nevertheless, there is a clear contrast enhancement from this simple operation.

We notice that the main disadvantage of denoising the squared magnitude image is that the noise variance (2) now becomes signal-dependent (see figure 2). Apart from that, assuming that the Gaussian approximation is valid, we can compare the SNR in the magnitude image with that in the squared magnitude image:

$$\begin{aligned} SNR_{mag} &= \frac{A^2}{\sigma^2} \\ SNR_{mag^2} &= \frac{A^4}{4\sigma^4\left(\frac{A^2}{\sigma^2}+1\right)} \\ &\approx \frac{1}{4} SNR_{mag} \end{aligned}$$

which means a 6dB decrease in SNR when working with the squared magnitude images compared to the magnitude image. Therefore, we propose a two-step denosing method, where we first remove the bias from the squared magnitude image using (3) and then apply denoising to the magnitude MRI image.

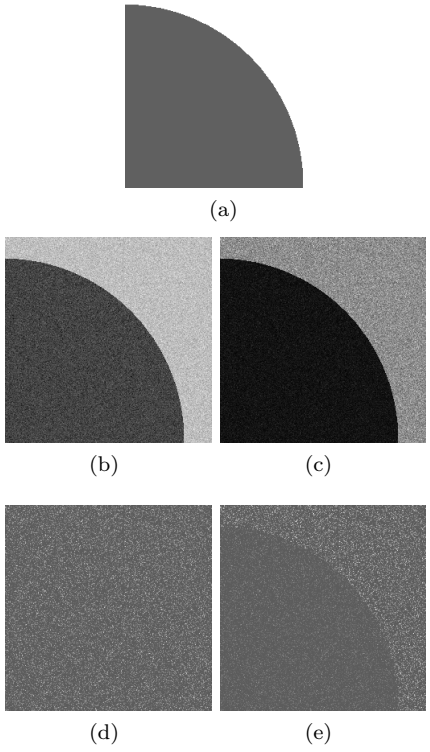

Figure 2: (a) Noiseless artificial signal consisting of a dark (low signal) area on a bright (high signal) background. (b) Noisy magnitude image. (c) Squared noisy magnitude image. (d) Difference between noisy and noiseless magnitude image. (e) Difference between squared noisy and squared noiseless magnitude image, note the signal-dependent noise variance.

3.2 Noise Removal

3.2.1 Empirical ProbShrink for white noise

In [10], a full-blind denoising algorithm was derived for different types of uncorrelated noise. This algorithm performs non-linear shrinkage on wavelet coefficients representing the signal. The noise model for a wavelet coefficient p at orientation o and scale s is:

$$y_{o,s}(p) = x_{o,s}(p) + n_{o,s}(p)$$

For compactness we drop the suffix o and index p. The idea behind the method is to divide the wavelet coefficients into two categories: wavelet coefficients that contain a signal of interest (hypothesis H_1) and wavelet coefficients that do not contain a signal of interest (hypothesis H_0). We will then approximate the MMSE estimate for x_s,

$$\hat{x}_s = E(x_s|y_s, H_1)P(H_1|y_s) + E(x_s|y_s, H_0)P(H_0|y_s),$$

making use of the assumptions:

1. $E(x_s|y_s, H_0) \approx 0$ as we expect no signal if there is no signal of interest present
2. $E(x_s|y_s, H_1) \approx y_s$ as we expect the signal of interest to be much higher than the noise level

This comes down to the estimator [10, 11]:

$$\hat{x}_s = P(H_1|y_s)y_s$$

After rewriting this as a generalized likelihood ratio, we get

$$\hat{x}_s = \frac{1}{1+\eta(y_s)\xi} y_s$$

with

$$\eta(y_s) = \frac{p_{Y|H}(y_s|H_0)}{p_{Y|H}(y_s|H_1)} \qquad \xi = \frac{P(H_0)}{P(H_1)} \tag{4}$$

These likelihood ratios (4) are then estimated empirically. The ratio ξ can be estimated from the significance map as the ratio of the amount of significant coefficients to the amount of insignificant coefficients:

$$\hat{\xi} = \frac{N - \sum_{p=1}^{N} S(y_s(p))}{\sum_{p=1}^{N} S(y_s(p))}$$

where $S(\cdot)$ is the significance label (see Section 3.2.2). $S(y) = 1$ means y is significant, and $S(y) = 0$ means y is insignificant. In [10], these significance labels were estimated by comparing interscale products to a threshold. Once the significance labels are established, the densities from (4) are estimated empirically. Due to instabilities in the tails, the likelihood ratio is evaluated by a piece-wise linear fit to its logarithm:

$$\log \hat{\eta(y_s)} \approx \begin{cases} a_1 + b_1 y_s & \hat{\eta(y_s)} < 1 \\ a_2 + b_2 y_s & \hat{\eta(y_s)} \geqslant 1 \end{cases} \tag{5}$$

Now we propose an extension of this method.

3.2.2 Extension for correlated noise

Since we want to remove correlated noise, we need to include noise correlation in the significance label. We propose:

$$S(y_s) = \begin{cases} 0 & ||\hat{\mathbf{y}}_{s+1}^t \mathbf{C}_n^{-\frac{1}{2}}||.||\mathbf{C}_n^{-\frac{1}{2}}\mathbf{y}_s|| \leq T \\ 1 & ||\hat{\mathbf{y}}_{s+1}^t \mathbf{C}_n^{-\frac{1}{2}}||.||\mathbf{C}_n^{-\frac{1}{2}}\mathbf{y}_s|| > T \end{cases} \tag{6}$$

where $\mathbf{y}$ represents a $N \times N$ neighborhood of wavelet coefficients, around the coefficient y, converted to a $1 \times N^2$ vector and $\mathbf{C}_n^{1/2}$ is the symmetric square root of $\mathbf{C}_n$. The measure combines the whitening properties of the noise covariance matrix $\mathbf{C}_n^{-1/2}$ on a vector of neighboring wavelet coefficients $\mathbf{y}_s$ surrounding the coefficient y_s [12], with multiscale edge propagation [10, 7] to detect significant wavelet coefficients. Figure 3 shows the power of the vector-based significance measure; most of the correlated noise that was incorrectly labeled as significant signal, by a measure that works on individual wavelet coefficients, is now labeled as insignificant. For this significance measure, we need an estimate of the noise covariance matrix $\mathbf{C}_n$ in every subband. This is done by estimating the noise power spectrum $P(e^{\frac{j2\pi k}{N}}, e^{\frac{j2\pi l}{N}})$ in the pixel domain, in a region outside the signal. Then, we apply the wavelet filters in the Fourier domain $H_{o,s}(e^{\frac{j2\pi k}{N}}, e^{\frac{j2\pi l}{N}})$, with s

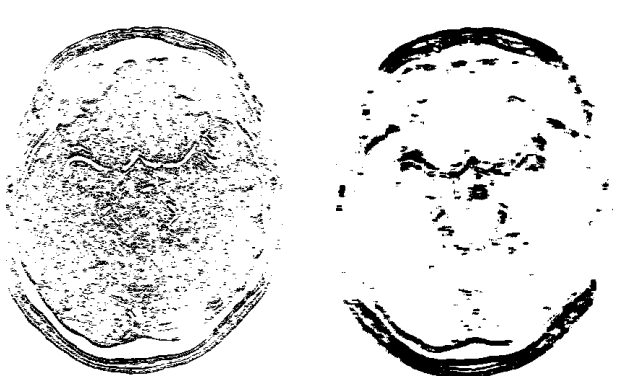

(a) (b)

Figure 3: comparison between: (a) a significance measure that works on individual coefficients from [10] and (b) our vector-based significance measure.

being the scale and o the orientation. To obtain the noise autocorrelation in each wavelet subband, we use the Wiener-Khinchin theorem:

$$R_{o,s}(m,n) = \text{IDFT}\left(P\left(e^{\frac{j2\pi k}{N}}, e^{\frac{j2\pi l}{N}}\right)\left|H_{o,s}\left(e^{\frac{j2\pi k}{N}}, e^{\frac{j2\pi l}{N}}\right)\right|^2\right)$$

Following the definition of the autocorrelation, elements of the noise covariance matrix $\mathbf{C}_n$ can be easily found.

4. RESULTS

In this Section, we compare the performance of the proposed algorithm with other existing techniques. We used a non-decimated wavelet transform with the two vanishing moments Daubechies wavelet. We used 5×5 windows and a threshold value T of 4 for the significance measure, note that the desired amount of noise suppression can be controlled very easily by varying this parameter T. Figure 4 show a clear visual improvement by the proposed algorithm over existing MRI denoising techiques [4, 10], as those are not designed for correlated noise. We also compared to BLS_GSM [13], a more general denoising algorithm that can handle correlated Gaussian noise. For the BLS_GSM algorithm's input parameters, we used the empirically estimated noise power spectrum and $\hat{\sigma} = \sqrt{\frac{1}{2N}\sum_{i=1}^{N} M_i^2}$ [5] as estimate for the approximated Gaussian distribution's noise standard deviation. Figure 4(d) shows the presented method. The difference is clear with figure 4(b): the versatile method from [10] leaves much of the noise untouched as it incorrectly detects too many significant wavelet coefficients which leads to too conservate shrinkage factors. Figure 4(c) (BLS_GSM from [13]) on the other hand, shows problems with oversmoothing. It also leaves the Rician bias untouched. As a consequence, the darkest parts of the image appear somewhat less dark and the tissue contrast is reduced.

We also compared these techniques on an image with artificial Rician correlated noise. Results can be checked visually on figure 5, table 1 shows the resulting PSNR. Table 1 shows a decrease in PSNR for the unaltered

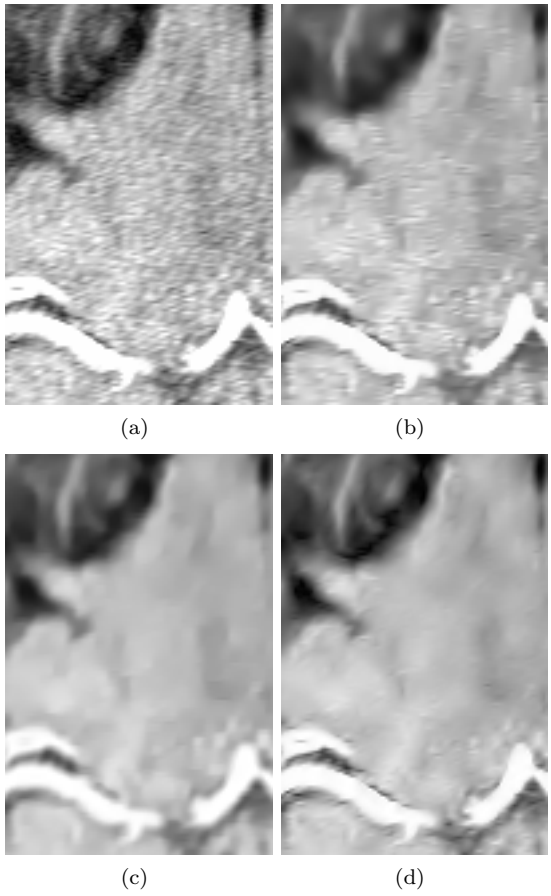

(a) (b)

(c) (d)

Figure 4: Visual denoising results for cropped parts of a real TOF-MRI dataset for different denoising methods: (a) noisy MRI magnitude image (b) versatile wavelet-based MRI denoising method from [10] (c) wavelet-based denoising method BLS_GSM from [13] (d) Proposed method.

BLS_GSM method. This is because the bias in the signal-less regions is not removed and accumulates into a very bad PSNR value. We therefore introduced the bias correction explained in Section 3.1 to this algorithm. The resulting increase in PSNR is indicative for the power of the simple bias correction technique. We also notice the oversmoothing on the image processed by BLS_GSM (figure 5(d)). Visual improvement can be achieved by heuristically scaling down the noise standard deviation parameter (figure 5(e)).

5. CONCLUSION

This paper presented a technique for removal of correlated Rician noise in MRI. Centered around a new significance measure to detect wavelet coefficients containing signal, the technique shows an advantage over existing white noise MRI denoising methods. We also presented a simple, yet highly effective way to suppress the signal-dependent bias introduced by Rician noise in low SNR regions. Due to the similarity of Rician noise to Gaussian noise in areas with high SNR, it should not surprise that the bias supression technique improves denois-

ing performance considerably, when combined with denoising algorithms for Gaussian noise. We also showed that, although bias supression is easier, operating on the squared magnitude MRI image is not desirable for denoising purposes as it decreases SNR considerably as well as introducing a signal-dependent noise variance.

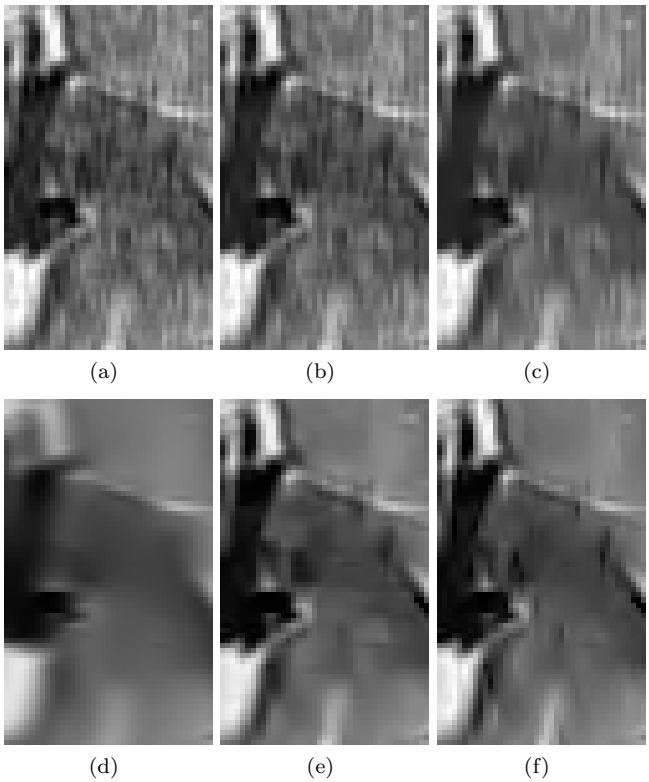

(a) (b) (c)

(d) (e) (f)

Figure 5: Visual denoising result for different methods: (a) MRI magnitude image with artificial correlated noise (b) wavelet-based MRI denoising method from [4] (c) versatile wavelet-based MRI denoising method from [10] (d) wavelet-based denoising method BLS_GSM from [13] with the bias correction from Section 3.1 (e) BLS_GSM with heuristically scaled down σ parameter (f) Proposed method.

Table 1: PSNR comparison for images in figure 5

Algorithm	PSNR
original noisy image	18.6dB
Nowak MRI	19.1dB
Versatile MRI	19.2dB
BLS_GSM	17.8dB
BLS_GSM with bias correction	25.2dB
proposed method	27.5dB

REFERENCES

[1] L. Landini, V. Positano, and M. F. Santarelli, eds., *Advanced Image Processing for MRI*. CRC press, 2005.

[2] M. A. Bernstein, D. M. Thomasson, and W. H. Perman, "Improved detectability in low SNR MR images by means of phase-corrected real construction," *IEEE Transactions on Image Processing*, vol. 16, pp. 813–817, March 1989.

[3] J. Sijbers, A. J. den Dekker, P. Scheunders, and D. V. Dyck, "Maximum-likelihood estimation of Rician distribution parameters," *IEEE Transactions On Medical Imaging*, vol. 17, pp. 357–361, June 1998.

[4] R. Nowak, "Wavelet-based rician noise removal for magnetic resonance imaging," *IEEE Transactions on Image Processing*, vol. 10, pp. 1408–1419, October 1999.

[5] J. Sijbers, *Signal and Noise Estimation from Magnetic Resonance Images*. PhD thesis, University of Antwerp, 1998.

[6] S. P. Awate and R. T. Whitaker, "Feature-preserving MRI denoising: A nonparametric empirical bayes approach," *IEEE Transactions On Medical Imaging*, vol. 26, pp. 1242–1255, September 2007.

[7] P. Bao and L. Zhang, "Noise reduction for magnetic resonance images via adaptive multiscale products thresholding," *IEEE Transactions on Medical Imaging*, vol. 22, pp. 1089–1099, September 2003.

[8] M. Alexander, R. Baumgartner, A. Summers, C. Windischberger, M. Klarhoefer, E. Moser, and R. Somorjai, "A wavelet-based method for improving signal-to-noise ratio and contrast in MR images," *Magnetic Resonance Imaging*, vol. 18, pp. 169–180, February 2000.

[9] M. Abramowitz and I. A. Stegun, *Handbook of Mathematical Functions*. New York: Dover, ninth dover printing, tenth GPO printing ed., 1964.

[10] A. Pižurica, W. Philips, I. Lemahieu, and M. Acheroy, "A versatile wavelet domain noise filtration technique for medical imaging," *IEEE Transactions on Medical Imaging*, vol. 22, pp. 323–331, March 2003.

[11] A. Pižurica and W. Philips, "Estimating the probability of the presence of a signal of interest in multiresolution single- and multiband image denoising," *IEEE Transactions on Image Processing*, vol. 15, pp. 654–665, March 2006.

[12] B. Goossens, A. Pižurica, and W. Philips, "Removal of Correlated Noise by Modeling Spatial Correlations and Interscale Dependencies in the Complex Wavelet Domain," in *IEEE Int. Conf. on Image Processing (ICIP)*, (San Antonio, Texas, USA), pp. 317–320, sept 2007.

[13] J. Portilla, V. Strela, M. J. Wainwright, and E. P. Simoncelli, "Image denoising using scale mixtures of gaussians in the wavelet domain," *IEEE Transactions On Image Processing*, vol. 12, pp. 1338–1351, November 2003.